JOC The Journal of Organic Chemistry

Article

pubs.acs.org/joc

Perylene-Derived Triplet Acceptors with Optimized Excited State Energy Levels for Triplet–Triplet Annihilation Assisted Upconversion

Xiaoneng Cui,[†] Azzam Charaf-Eddin,[‡] Junsi Wang,[†] Boris Le Guennic,[§] Jianzhang Zhao,*[,†] and Denis Jacquemin*[,‡,∥]

[†]State Key Laboratory of Fine Chemicals, School of Chemical Engineering, Dalian University of Technology, E-208 West Campus, 2 Ling-Gong Road, Dalian 116024, P. R. China

[‡]CEISAM UMR CNRS 6230, Université de Nantes, 2 rue de la Houssinière, BP 92208,44322Nantes Cedex 3, France

[§]Institut Universitaire de France (IUF), 103, Boulevard Saint-Michel, 75005 Paris Cedex 05, France

[∥]Institut des Sciences Chimiques de Rennes, UMR 6226 CNRS-Université de Rennes 1, 263 Av. du General Leclerc, 35042 Rennes Cedex, France

Supporting Information

ABSTRACT: A series of perylene derivatives are prepared as triplet energy acceptors for triplet–triplet annihilation (TTA) assisted upconversion. The aim is to optimize the energy levels of the T_1 and S_1 states of the triplet acceptors, so that the prerequisite for TTA ($2E_{T1} > E_{S1}$) can be better satisfied, and eventually to increase the upconversion efficiency. Tuning of the energy levels of the excited states of the triplet acceptors is realized either by attaching aryl groups to perylene (via single or triple carbon–carbon bonds), or by assembling a perylene-BODIPY dyad, in which the components present complementary S_1 and T_1 state energy levels. The S_1 state energy levels of the perylene derivatives are generally decreased compared to perylene. The anti-Stokes shift, TTA, and upconversion efficiencies of the new triplet acceptors are improved with respect to the perylene hallmark. For the perylene-BODIPY dyads, the fluorescence emission was substantially quenched in polar solvents. Moreover, we found that extension of the π-conjugation of BODIPY energy donor significantly reduces the energy level of the S_1 state. Low S_1 state energy level and high T_1 state energy level are beneficial for triplet photosensitizers.

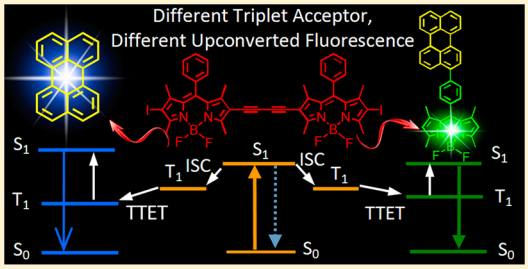

INTRODUCTION

Triplet–triplet-annihilation (TTA) assisted upconversion has attracted much attention, due to its advantages over the conventional upconversion methods: strong absorption of the excitation, low excitation power threshold (noncoherent, solar light is sufficient), and high upconversion quantum yields (up to 20%).[1−12] Moreover, the TTA assisted upconversion is based on supramolecular features, i.e., intermolecular energy transfer between the triplet photosensitizer and the triplet acceptor. The triplet photosensitizer (energy donor) and the triplet energy acceptor/emitter involved in TTA assisted upconversion can be selected independently. Consequently, both the excitation and emission wavelengths of a TTA assisted upconversion protocol can be readily changed by combining different triplet photosensitizers and triplet acceptors (emitters).[2] This feature differs from other upconversion methods, such as those based on rare earth materials, for which the excitation/emission wavelengths are not easily tunable.[13−17] Recently, TTA assisted upconversion has been widely used in luminescent bioimaging or oxygen (O_2) sensing,[18−20] solar cells,[21−23] and photocatalysis including hydrogen (H_2) production by water photolysis.[24]

The photophysical properties of triplet photosensitizers and triplet acceptors/emitters are crucial for TTA assisted upconversion. An ideal triplet photosensitizer should show strong visible light absorption, long-lived triplet excited state, and appropriate T_1 state energy level.[25−27] For the triplet acceptor, the desired photophysical properties include high fluorescence quantum yield, appropriate T_1 state energy level (*lower* than the T_1 state energy level of the triplet photosensitizers), but *higher* S_1 state energy level than the triplet photosensitizer, to ensure the TTA assisted upconversion, i.e., upconverted fluorescence with anti-Stokes shift against the incident excitation light. Furthermore, the crucial photophysical property for triplet energy acceptor is $2E_{T1} > E_{S1}$, which is required for efficient TTA process.[25,26,28]

Currently, most studies devoted to TTA assisted upconversion have been focused on the application in different inert matrixes, such as nanoparticles or polymeric microcapsules, or focus on development of new triplet photosensitizers, but the triplet acceptors are rarely investigated.[29−43] However, the selection of an appropriate triplet acceptor is crucial and far

Received: December 7, 2013
Published: February 11, 2014

Scheme 1. Synthesis of the Organic Triplet Acceptor[a]

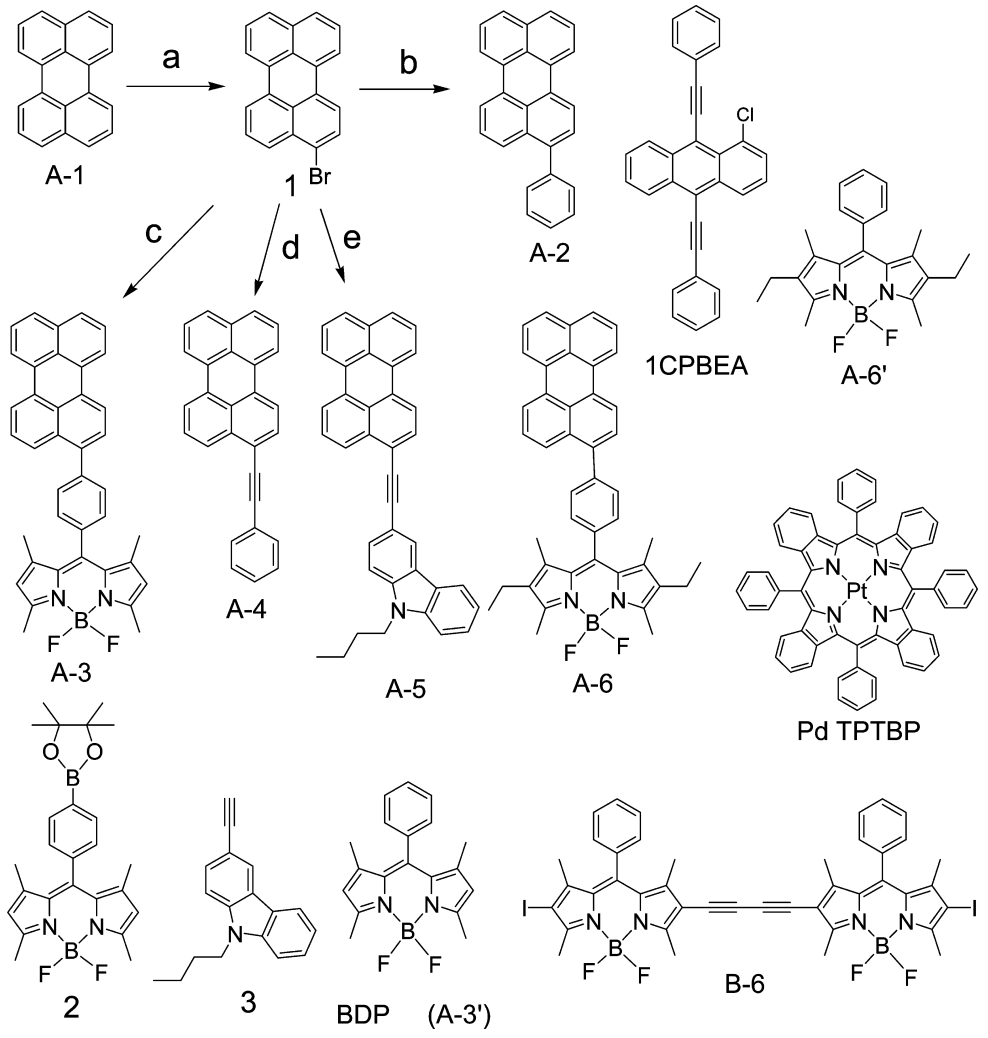

[a]Triplet acceptors **A-1**−**A-6**, 1-chloro-bis-phenyl ethynylanthracene (1CPBEA), BDP (**A-3′**), and the triplet sensitizers **B-6**, PdTPTBP are presented. Compound **1**,[46] **2**,[47] and **3**[42] were reported previously. (a) NBS, DMF, r.t., 20 h; yield: 84%; (b) Phenylboronic Acid, K_2CO_3, $Pd(pph_3)_4$, toluene/ethanol/H_2O (2:2:1 v/v/v), 80 °C, under Ar, reflux, 8 h; yield: 72%; (c) compound **2**, K_2CO_3, $Pd(pph_3)_4$, toluene/ethanol/H_2O (2:2:1 v/v/v), 80 °C, under Ar, reflux, 8 h; yield: 40%; (d) phenylacetylene, $(pph_3)_2PdCl_2$, pph_3, CuI, Et_3N, 90 °C, under Ar, reflux, 8 h; yield: 55%; (e) 9-butyl-3-ethynyl-carbazole (**3**), $(pph_3)_2PdCl_2$, pph_3, CuI, Et_3N, 90 °C, under Ar, reflux, 8 h; yield: 47%.

from being a trivial task, due to the desired photophysical properties mentioned above, one of the major concerns being to satisfy the $2E_{T1} > E_{S1}$ prerequisite.[5] Unfortunately the vast majority of available triplet acceptors only satisfy this requirement marginally. For example, perylene is a versatile chromophore and has been widely used as triplet acceptor for TTA assisted upconversion.[2,5] However, the S_1 and T_1 state energy levels of perylene are 2.78 and 1.53 eV, respectively. Therefore, the TTA of perylene is assumed to be poor. In order to overcome this limitation, a hetero BODIPY-perylene dimer triplet acceptor was reported recently, in which the perylene unit acts as the triplet energy acceptor, but the BODIPY part allowed a reduction of the S_1 state energy.[28] As a result, the TTA of the dyad acceptor was improved compared to the unsubstituted perylene because the $2E_{T1} > E_{S1}$ requirement could be better satisfied. As a result, improved TTA assisted upconversion efficiency was observed with this hetero chromophore dimer.[28] However, much room is left to fully explore this novel strategy for designing more efficient triplet energy acceptors. For example, although intramolecular energy transfer may be dominant for the hetero chromophore dimer, intramolecular electron transfer cannot be excluded. Intramolecular electron transfer could be detrimental for the fluorescence of the dyad triplet acceptor. Moreover, with a significantly red-shifted upconverted emission, the anti-Stokes shifts of the TTA assisted upconversion that has been obtained with the previously reported perylene-BODIPY dyad was largely compromised compared with its single perylene counterpart.[28] Normally large anti-Stokes shift is desired for TTA assisted upconversion.[44] Therefore, it is interesting to explore new triplet acceptors with balanced upconversion performances, such as improved TTA efficiency, and at the same time, fairly large anti-Stokes shift.

Herein, a series of perylene-based triplet acceptor/emitters has been prepared by attaching aryl groups to perylene (via single or triple carbon−carbon bonds) or constructing BODIPY-perylene dyads. The fluorescence emission of these perylene derivatives is red-shifted as compared to perylene and the energy of the S_1 state is decreased compared to perylene, which is beneficial for TTA. For the TTA assisted

dx.doi.org/10.1021/jo402718e | J. Org. Chem. 2014, 79, 2038−2048

upconversion, we obtained generally improved TTA efficiency with these new triplet acceptors. We demonstrated that for the perylene-BODIPY dimers, the fluorescence was substantially quenched in polar solvents. This property was not found for the respective components of the dyads, i.e., the perylene or BODIPY chromophores. Furthermore, the energy level of the S_1 state of BODIPY triplet photosensitizer was substantially decreased by extension of the π-conjugation framework (the fluorescence emission wavelength is red-shifted), whereas the T_1 energy did not decrease substantially. These results are useful for the design of new triplet photosensitizers and acceptors for TTA assisted upconversion, as well as for the study of photochemistry and photophysics of organic chromophores.

RESULTS AND DISCUSSION

2.1. Design and Synthesis of the Perylene/Bodipy Based Dyad Triplet Acceptors. Two strategies were used for designing perylene-based triplet acceptors with the aim to improve the TTA efficiency by optimization of the S_1 and T_1 state energy levels. First, the π-conjugation framework of perylene was extended by introducing aryl moieties, which are linked to the perylene framework by C≡C triple bond (**A-4**, **A-5**, Scheme 1). The fluorescence emission wavelength of these perylene derivatives is expected to be red-shifted as compared to perylene;[45] in other words, the S_1 state energy level of these derivatives will be lower than that of perylene. As a result, the $2E_{T1} > E_{S1}$ relation can be better satisfied and the TTA can be improved compared to perylene.[28] Second, with the preparation of a new perylene-BODIPY dimer triplet acceptor, BODIPY was selected as the fluorescence emitter due to its satisfactory photophysical properties, e.g., high fluorescence quantum yields and environmentally independent fluorescence emission.[48−52] The fluorescence emission property of the hetero chromophore dimers is more complex than the respective components of the dyads; for example, the fluorescence emission intensity of the dyads is highly sensitive to the polarity of the solvents, which is different from the property of the perylene or the BODIPY chromophores alone.

The reactions were carried out with 1-bromoperylene as the starting material (Scheme 1). Pd(0)-catalyzed Suzuki crossing coupling and Sonogashira coupling reactions were used. All the compounds were obtained with satisfactory yields.

2.2. UV−vis Absorption and Fluorescence Emission Spectra. The UV−vis absorption spectra of the compounds were studied (Figure 1). Auxochromic groups have a noticeable impact on the perylene spectra. For example, attaching the phenylethynyl moiety to the perylene (**A-4**) induces a red-shifted absorption maximum at 467 nm (439 nm for perylene). Similar bathochromic shifts were observed for other derivatives.

For the perylene-BODIPY dimer, **A-3**, besides the absorption bands of the perylene core, a distinct absorption band at 504 nm was observed, which is attributed to the BODIPY moiety. The absorption profile indicates weak electronic interaction between the perylene and the BODIPY part at the ground state (see also the later calculations second).[53,54] With 2,6-diethyl substituent on the BODIPY core, **A-6**, the absorption is further red-shifted. Clearly in both **A-3** and **A-6**, the S_1 energy level is lower than that of perylene.

The fluorescence emission spectra were recorded (Figure 2). All the perylene derivatives show red-shifted fluorescence emission compared to perylene, confirming that the S_1 energy level of the derivatives is decreased, a beneficial shift for TTA

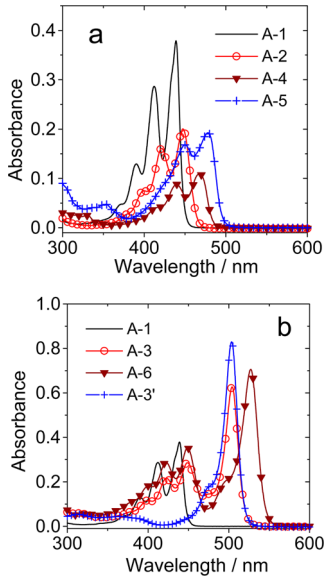

Figure 1. UV−vis absorption spectra of the compounds. In toluene. $c = 1.0 \times 10^{-5}$ M, 20 °C.

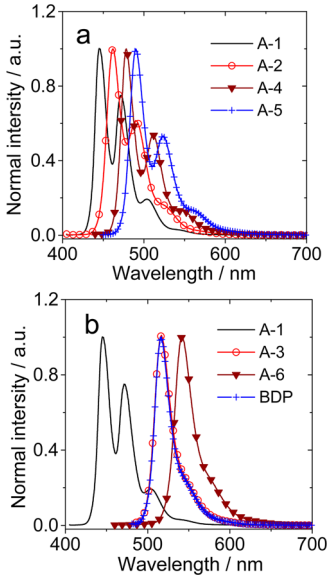

Figure 2. Normalized fluorescence emission spectra of (a) **A-1** (λ_{ex} = 400 nm), **A-2** (λ_{ex} = 400 nm), **A-4** (λ_{ex} = 435 nm), and **A-5** (λ_{ex} = 444 nm); and (b) **A-1** (λ_{ex} = 400 nm), **A-3** (λ_{ex} = 480 nm), **A-6** (λ_{ex} = 449 nm), and BDP (λ_{ex} = 480 nm). $c = 1.0 \times 10^{-5}$ M in toluene, 20 °C.

enhancement. With the introduction of the carbazole moiety through the C≡C triple bond linker (**A-5**), a strongly red-shifted emission at 490 nm is obtained, and we attribute this feature to the charge-transfer (CT) nature of the compound. All the new perylene derivatives show blue-shifted fluorescence emission compared to the previously reported BODIPY-perylene dimer (**A-6**) and the same holds for **A-3** that emits at 517 nm (25 nm blue shift). These increased S_1 state energy levels are beneficial for reaching larger anti-Stokes shift.[28]

The solvent dependency of the UV−vis absorption and the fluorescence emission spectra were also assessed (Figure 3). **A-3** shows similar UV−vis absorption in solvents of different polarity (hexane, toluene, THF, and MeCN), indicating that the ground state of **A-3** is not affected by the polarity of the

dx.doi.org/10.1021/jo402718e | J. Org. Chem. 2014, 79, 2038−2048

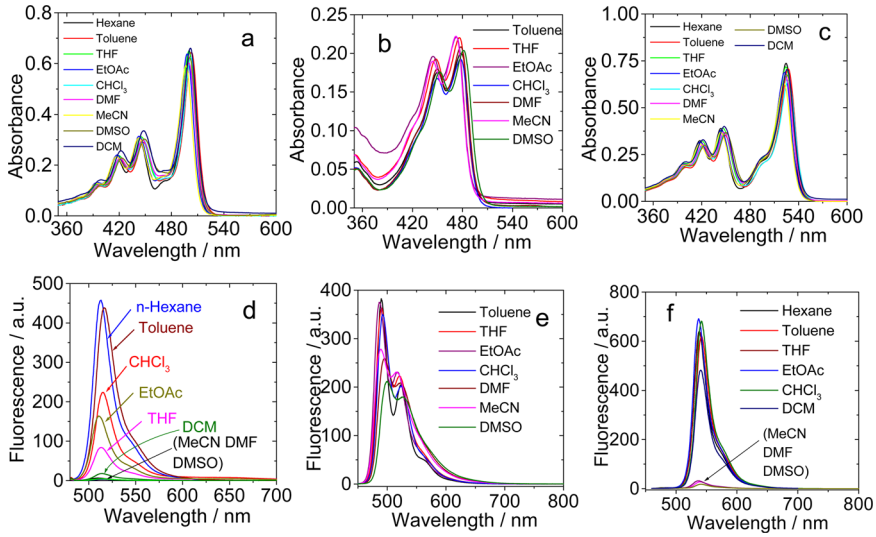

Figure 3. UV−vis absorption spectra of (a) **A-3**, (b) **A-5**, and (c) **A-6** in different solvents. $c = 1.0 \times 10^{-5}$ M, 20 °C. Emission spectra of (d) **A-3** (λ_{ex} = 480 nm), (e) **A-5** (λ_{ex} = 444 nm), (f) **A-6** (λ_{ex} = 449 nm) in different solvents. $c = 1.0 \times 10^{-5}$ M, 20 °C.

Table 1. Photophysical Parameters of the Organic Triplet Acceptor

	λ_{abs}[a] (nm)	ε[b]	λ_{ex} (nm)	λ_{em} (nm)	Φ[c]	τ_F[d] (ns)
BDP (**A-3′**)	503	8.30	480	516	0.72[g]	3.73\3.30[e]\3.42[f]
A-1	412\439	2.87\3.82	400	445\471\504	0.98	3.80
A-2	421\447	1.61\0.20	400	462\490	0.94	3.26
A-3	423\449\504	2.16\2.86\6.28	480	517	0.58	2.97\3.80[e]\3.64[f]
A-4	440\467	0.88\1.09	435	478\511\546	0.68	2.35
A-5	450\478	1.68\1.93	444	490\526	0.64	2.17
A-6	442\449\527	2.88\3.53\7.07	449	542	0.75	4.86\4.83[e]\5.16[f]

[a]In toluene (1.0×10^{-5} M), 20 °C. [b]Molar extinction coefficient at the absorption maxima. ε: 10^4 M^{-1} cm^{-1}. [c]Fluorescence quantum yields in toluene, with perylene as the standard (Φ_F = 98% in *n*-hexane). [d]Fluorescence lifetimes in toluene. [e]In THF. [f]In EtOAc. [g]Literature value.[43]

solvent. Similar results were observed for other compounds, such as **A-5** and **A-6**.

Interestingly, the emission shows a drastically different response to the solvent polarity, e.g., the emission intensity decreases in polar solvents, such as DMSO and MeCN compared with that in less polar solvents, such as toluene and THF. For **A-5**, this effect is moderate and can be attributed to the CT feature. Contrary to **A-5**, the fluorescence intensity of dyad **A-3** is highly dependent on the solvent polarity (Figure 3d): it fluoresces intensively in nonpolar solvents, such as hexane and toluene, but the emission is much weaker in THF and ethyl acetate. The emission band shape remains the same. In polar solvents (MeCN, DMF, and DMSO), the fluorescence emission is almost completely quenched. The quenched fluorescence of **A-3** in polar solvents is not related to solubility, as normal UV−vis absorption spectra were observed for **A-3** in these solvents. We tentatively attribute the quenching to the photoinduced intramolecular electron transfer, which is known to be more efficient in highly polar solvents.[54,55] This interpretation is confirmed by the fluorescence emission of BODIPY in different solvents, for which no polarity-dependent fluorescence emission was observed (Figure S16).

For **A-6**, similar solvent polarity-dependent fluorescence emission was observed (Figure 3f), but with a more distinct ON−OFF character, that is, the fluorescence emission is hardly affected when going from nonpolar and slightly polar solvents, but is completely switched off in highly polar media. We emphasize that similar solvent-polarity induced fluorescence quenching was observed by excitation of either the perylene part or the BODIPY part (Figure S18). We measured the nanosecond time-resolved transient difference absorption of both **A-3** and **A-6**, but no signal was detected, hinting that triplet excited state was produced by neither the charge transfer nor the charge recombination, or that the charge separated state is short-lived (less than 10 ns, based on the time-resolution of the transient absorption spectrometer).[55]

The photophysical properties of the compounds were listed in Table 1. All the perylene derivatives show smaller fluorescence quantum yields than perylene. The fluorescence lifetimes in toluene are close to that of perylene. In polar solvent such as THF, however, the fluorescence lifetime of **A-3** and **A-6** does not decrease. Thus, static quenching or formation of ground state complex in polar solvents are responsible for the quenching.

2.3. DFT Calculations. Time-dependent density functional theory (TD-DFT) simulations have been performed on the two dyads, as well as on model systems for the BODIPY and perylene moieties. Details of the computational models can be found in the Experimental Section.[56−65] The obtained energetic diagram, together with representation of the excited states, can be found in Figure 4. Consistently with experiments, one notices that the lowest excited-state, ES1, is clearly BODIPY-centered, whereas the second, ES2, that lies slightly higher in energy is characteristic of the perylene group. Following Kasha's rule (the process can also be considered as intramolecular energy transfer) and considering that ES1 and ES2

dx.doi.org/10.1021/jo402718e | J. Org. Chem. 2014, 79, 2038−2048

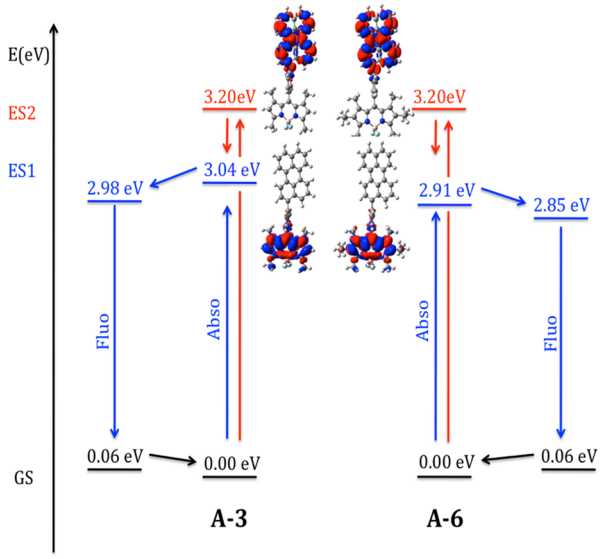

Figure 4. Energetic diagram obtained at the SS-PCM M06-2X/6-31G(d) level for the two BODIPY-perylene dyads. For the vertical absorption, representation of density difference plots (contour thresholds of 0.0004 a.u., blue/red regions: decrease/increase of density upon transition) are also given. Energies represented are not corrected for vibrational effects; see Experimental Section for more details.

are close in energy, it is therefore expected that only the emission signature of the BODIPY can be detected, and this is consistent with the experiments. This was further confirmed by additional calculations. First, the computations performed on the compounds yield vertical absorption energies of 3.04, 2.94, and 3.23 eV for **A-3′**, **A-6′**, and **A-2**, respectively, which obviously correspond to the 3.04, 2.91, and 3.20 eV values reported in Figure 4. Second, we have determined the vibrationally resolved spectra with TD-DFT and it turns out that the hallmark BODIPY/perylene band topologies are restored, so that it is obvious that the experimental absorption spectra of **A-3** is the addition of **A-3′** and **A-2**, whereas its emission is similar to that of **A-3′** (Figure 5). Third, we have computed 0−0 energies for **A-3** and **A-6** using a reliable TD-DFT protocol that accounts for both state-specific solvation and vibrational effects.[57] The obtained values of 2.86 and 2.72 eV, that after simple linear corrections (see Section 3.1 in ref 56) yield 2.46 and 2.33 eV, which fit experimental values of 2.43 and 2.32 eV very well.

2.4. Electrochemical Properties. The electrochemical properties of the dyad triplet acceptors were studied with cyclovoltametry (CV, Figure 6). A reversible oxidation was observed at $E_{1/2}$ = +0.89 V, which is anodically shifted by 0.04 V compared with perylene (+0.93 V) for **A-2**. This result indicates that attachment of the phenyl ring to the perylene section perturbs the electronic property of the latter. The CV of the **A-6** was also studied (Figure 6). Beside the reversible oxidation peak at +0.98 V, a pseudoreversible reductive band at $E_{1/2}$ = −1.40 V was observed, which can be attributed to the reduction of the BODIPY section in **A-6**, a postulate supported by electrochemical data of reference compounds (Table 2).

The free energy changes of the PET were calculated according to the Rehm−Weller equation (Table 2; for the computational details, please refer to the Supporting Information). They are small, which indicates that the PET is weakly allowed. This interpretation is in agreement with the

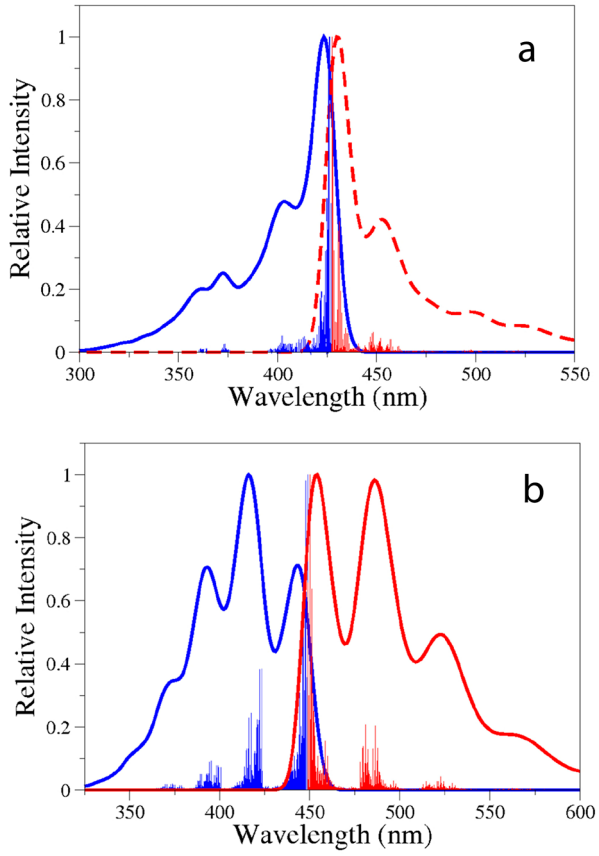

Figure 5. Vibronic spectra computed for **A-3′** (left) and **A-2** (right).

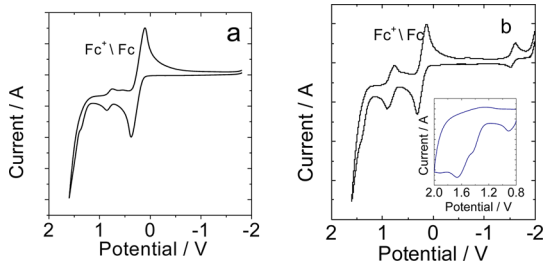

Figure 6. Cyclic voltammogram of the triplet acceptor (a) **A-2** and (b) **A-6**. Ferrocene (Fc) was used as reference $E_{1/2}$ = +0.38 V (Fc^+/Fc) vs SCE (saturated calomel electrode). Inset: (b) Note there is no apparent oxidation peak of 2-ethyl-BDP. In deaerated CH_2Cl_2 solutions containing 1.0 mM acceptor alone, or with ferrocene, 0.10 M $Bu_4N[PF_6]$ as supporting electrolyte, $Ag/AgNO_3$ reference electrode, scan rates: 100 mV/s.

experimental fact that the fluorescence of the dyad triplet acceptors is only quenched in highly polar solvents, especially for **A-6** (Figure 3f). PET is more efficient in polar solvents because of the increased free energy changes.

2.5. TTA Assisted Upconversion with the Perylene Derivatives as the Triplet Acceptor. The perylene derivatives were used as triplet acceptors for TTA assisted upconversion. **B-6** was used as triplet photosensitizer, for which the absorption is red-shifted compared with the perylene derivatives, but the T_1 state energy level of **B-6** is higher than that in perylene derivatives. This energy level profile ensures the triplet−triplet energy transfer (TTET) from the triplet photosensitizer to the triplet acceptors.[43]

dx.doi.org/10.1021/jo402718e | J. Org. Chem. 2014, 79, 2038−2048

Table 2. Redox Potentials of Acceptors and the of Free-Energy Changes (ΔG_{ET}, PET) for the Potential Intramolecular Electron Transfer (with Perylene Unit as Electron Donor and BODIPY Unit as Electron Acceptor in A-3 and A-6)[a]

	$E_{(OX)}$ (V)	$E_{(RED)}$ (V)	ΔG_{cs}(eV)
BDP	+1.14	−1.66	[b]
A-1	+0.89	[b]	[b]
A-2	+0.93	[b]	[b]
A-3	+0.90	−1.49	0.18[c]/0.11[d]/−0.077[e]/−0.37[f]
A-6	+0.98	−1.40	0.69[c]/0.19[d]/0.003[e]/−0.29[f]

[a]Anodic and cathodic peak potential were presented. The potential values of the compounds are vs standard hydrogen electrode (with Fc as internal reference, for which $E_{1/2}$ (Fc^+/Fc) = +0.38 V vs SCE (saturated calomel electrode)). Cyclic voltammetry in Ar saturated CH_2Cl_2 containing a 0.10 M Bu_4NPF_6 supporting electrolyte; Counter electrode is Pt electrode; working electrode is glassy carbon electrode; $Ag/AgNO_3$ couple as the reference electrode. $c[Ag^+]$ = 0.1 M. 1.0 mM dyad photosensitizers in DCM, 20 °C. Conditions: 1.0 mM dyad photosensitizers and 1.0 mM ferrocene in DCM, 293 K, and calculated relative to SCE (saturated calomel electrode). [b]No reduction potential were observed, or no ΔG_{cs} values were calculated. [c]Value of ΔG_{cs} in toluene, with perylene unit as electron donor. [d]Value of ΔG_{cs} in $CHCl_3$, with perylene unit as electron donor. [e]Value of ΔG_{cs} in DCM, with perylene unit as electron donor. [f]Value of ΔG_{cs} in MeCN, with perylene unit as electron donor.

The TTA assisted upconversion with different triplet acceptors is given in Figure 7. With perylene as triplet acceptor

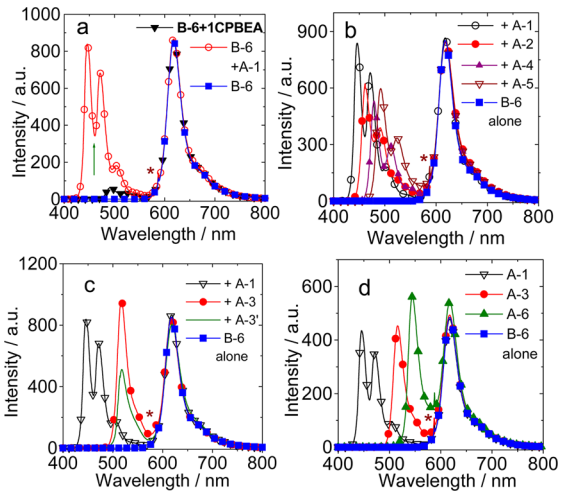

Figure 7. Upconversions with **B-6** as triplet photosensitizer and different triplet acceptors. (a) **A-1** and **1CPBEA**, (b) **A-1**, **A-2**, **A-4**, and **A-5**, (c) **A-1**, **A-3**, and **A-3′**. Excited with 589 nm continuous laser (4.8 mW, 24.5 mW cm^{-2}). (d) Emission of the sensitizers in the presence of triplet acceptor **A-1**, **A-3**, and **A-6**. Excited with 589 nm continuous laser (2.8 mW, 14.3 mW cm^{-2}). c [**B-6**] = 2.0×10^{-6} M; c [Acceptor] = 4.0×10^{-5} M. In deaerated toluene, 20 °C.

(**A-1**), intense upconverted fluorescence emission was observed, whereas with **A-2**, **A-4**, and **A-5**, a red-shifted emission was observed but with a weaker upconversion emission intensity than **A-1**. However, we have shown that the fluorescence quantum yields of the new perylene derivatives are smaller than their perylene counterpart. Considering this result, the TTA efficiency of the new triplet acceptors is actually exceeding the perylene (Table 3). The higher TTA efficiency of the new triplet acceptors can be attributed to their lower S_1 energy. It should be pointed out that the TTA is dependent on the excitation power; therefore, the TTA efficiencies reported in this paper cannot be compared directly with that reported previously.[28]

Next, the TTA assisted upconversion bands with **A-1**, **A-3**, and BODIPY (**A-3′**) as the triplet acceptor were compared (Figure 7c). For **A-3** and BODIPY (**A-3′**), the upconverted emission bands have the same shape and wavelength, which are red-shifted compared to perylene. This result indicates that the emissive singlet excited state of **A-3** is localized on the BODIPY part, not on perylene part. Furthermore, the TTA assisted upconversion with **A-3** is much larger than that obtained using BODIPY as the triplet acceptor. This enhanced TTA assisted upconversion with the dyad (**A-3**) is due to the improved TTET because the T_1 state energy level of perylene is lower than that of BODIPY. The upconversion emission intensity with **A-3** is comparable to that of perylene. However, it should be pointed out that the anti-Stokes shift of the TTA assisted upconversion with the new perylene-based triplet acceptor is smaller than that with perylene as the triplet acceptor; this is within expectation since the S_1 state energy level is lower than that of perylene.

Previously it was reported that TTA can be improved using **A-6** as triplet acceptor/emitter rather than perylene.[28] However, the anti-Stokes shift with **A-6** is smaller than that with perylene. With **A-3** as the triplet acceptor, the anti-Stokes shift (74 nm) is increased with respect to **A-6** (46 nm).

We noted that the upconversion quantum yield of **B-6** with perylene as acceptor is up to 17%. In our previous report, the upconversion quantum yield with **1CPBEA** (Scheme 1) as triplet acceptor was 1%.[43] Our selection of **1CPBEA** as triplet acceptor was based on the assumption that the extended π-conjugation framework of BODIPY in **B-6** will yield a T_1 state with decreased energy level than BODIPY (**A-3′**). However, the present higher upconversion quantum yield with perylene as the triplet acceptor indicates that this may not be the case. That is, the T_1 *triplet* state energy level of **B-6** may be not significantly reduced compared with that of BODIPY, although the S_1 *singlet* state energy level of **B-6** is much lower than that of BODIPY (i.e., the fluorescence emission wavelength of **B-6** is 623 nm whereas that of BODIPY is 516 nm). This information is helpful for designing new triplet photosensitizers, since the current knowledge on the relationship between molecular structure and T_1 state energy level is very limited, at least for organic chromophores.[27]

In order to demonstrate the versatility of the triplet acceptors, a red light-excitable triplet photosensitizer PdTPTBP was also used for TTA assisted upconversion. A 635 nm red laser was used as the excitation source (Figure 8).[29] Similar upconversion results were observed (see parameters in Table 3). Notably all the new triplet acceptors show higher TTA efficiency than that with perylene.

In order to prove that the emission observed in the TTA assisted upconversion is genuine upconverted delayed fluorescence, the time-resolved emission spectra of the TTA assisted upconversion was studied (Figure 9).[66,67] The luminescence lifetime is much longer than the prompt fluorescence lifetime of the perylene-based triplet acceptors, therefore the TTA assisted upconversion was verified (Figure 10). For example, the prompt fluorescence lifetime of **A-3** attains 3.27 ns. In the TTA assisted upconversion experiments, the lifetime of the delayed fluorescence is up to 292.2 μs.

dx.doi.org/10.1021/jo402718e | J. Org. Chem. 2014, 79, 2038−2048

Table 3. Upconversion Parameters of B-6, PdTPTBP with Triplet Acceptor A-1−A-6 and A-3′

		A-1	A-2	A-3	A-4	A-5	A-6	A-3′
B-6[a]	Φ_{UC} (%)[b]	17.8	11.1	10.9	7.9	10.5	15.1[g]	6.3
	Φ_{TTA}(%)[c]	4.7	5.9	9.8	6.4	9.4	6.0[g]	8.7
	K_{sv}[d]	465.9	240.8	233.6	221.3	245.7	396.8	117.6
	τ_{DF} (μs)[e]	230.7	207.6	292.2	257.3	217.1	330.2	211.6
PdTPTBP[f]	Φ_{UC}	7.2	10.4	8.1	5.0	5.3	11.7	-
	Φ_{TTA}	3.3	5.8	7.0	6.0	4.3	8.2	-

[a]Excited with 589 nm laser (4.8 mW), with the prompt fluorescence of **B-6** as the inner standard (Φ = 10.6% in toluene) and the concentration of sensitizers (**B-6**) is 2.0×10^{-6} M. *c* [Acceptor] = 4.0×10^{-5} M. [b]Upconversion quantum yield (Φ_{UC}). [c]Relative triplet−triplet annihilation yield (Φ_{TTA}) of **B-6** and PdTPTBP, the triplet−triplet-energy-transfer (TTET) efficient of BDP is approximated as 100%. [d]Stern−Volmer constants. In 10^3 M^{-1}. [e]Lifetimes of the delayed fluorescence (upconverted fluorescence). $\Phi_{UC} = \Phi_{ISC} \times \Phi_{TTET} \times \Phi_{TTA} \times \Phi_F$. [f]Excited with 635 nm laser, with the prompt fluorescence of H_2TPTBP as the standard (Φ = 0.28% in toluene) and the concentration of sensitizers (PdTPTBP) is 2.0×10^{-6} M. *c* [Acceptor] = 4.0×10^{-5} M; in deaerated toluene, 20 °C. [g]Using **A-3** as TTA upconversion quantum yield reference, calculated with the upconverted fluorescence emission peak area upon excitation with laser at power of 2.8 mW.

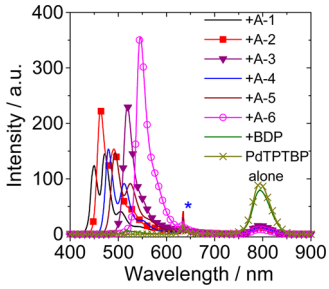

Figure 8. Upconversions with photosensitizer **PdTPTBP**. Emission of the sensitizer in the presence of triplet acceptor **A-1**, **A-2**, **A-3**, **A-4**, **A-5**, **A-6**, and **BDP**. Excited with 635 nm laser (4.8 mW, 17.0 mW cm^{-2}). (*c* [PdTPTBP] = 2.0×10^{-6} M; *c* [acceptor] = 4.0×10^{-5} M; in deaerated toluene, 20 °C).

In order to study the TTET efficiency between the triplet photosensitizer **B-6** and the proposed triplet acceptors, the Stern−Volmer quenching curves were plotted (Figure 11). The quenching results clearly indicate that the perylene based triplet acceptors are all more efficient than BODIPY as triplet quencher, presumably due to the lower T_1 state energy level of the new perylene based triplet acceptors compared with BODIPY. Among the perylene based triplet acceptors, **A-1** and **A-6** are the most efficient. The other perylene based triplet acceptors give similar quenching constants. We tentatively attribute these results to the bulkiness of the different derivatives (diffusion limited bimolecular quenching ability may be affected) and the different redox potentials (Dexter triplet energy transfer may be affected). A more detailed study is underway.

The TTA assisted upconversion with the perylene-based triplet acceptors is visible to unaided eyes (Figure 12). For the triplet photosensitizer **B-6** alone, red emission was observed, which is attributed to the fluorescence of **B-6** at 623 nm. In the presence of triplet acceptors such as **A-1**, **A-2**, **A-4**, **A-5**, and so forth, a panel of emission colors from purple, pink to yellow could be observed (Figure 12). These different emission colors are due to the different delayed fluorescence emission wavelength of the triplet acceptors, i.e., the different anti-Stokes shifts of the TTA assisted upconversion. Such a tuneability of the TTA assisted upconversion wavelength with a library of triplet acceptor is reported here for the first time.

2.6. Conclusions. In summary, aiming to optimize the relevant energy levels of the T_1 and the S_1 states of triplet acceptors to enhance the triplet−triplet annihilation (TTA) process and the TTA assisted upconversion efficiency, a series of perylene derivatives were prepared as triplet energy acceptors. To this end, approaches of attaching aryl groups to perylene (via single or triple carbon−carbon bonds) or assembling perylene-BODIPY dyads were used. It was found that the S_1 state energy levels are generally decreased. As a result the TTA was improved compared to perylene, the benchmark triplet acceptor widely used for TTA assisted upconversion. The photophysical properties of the triplet acceptors (anti-Stokes shift, TTA efficiency, and TTA assisted upconversion efficiency) are generally improved compared to that of perylene. Interestingly, we observed that the fluorescence of the perylene-BODIPY dyad triplet acceptors was diminished in polar solvents. Furthermore, we found that with extension of the π-conjugation framework of BODIPY, the S_1 state energy level decreases more substantially compared with the T_1 state energy level, which is ideal for BODIPY derivatives to be used as triplet photosensitizers. These results will be useful for the future molecular structural design of triplet photosensitizers and acceptors and for the study of the photochemistry of organic chromophores.

EXPERIMENTAL SECTION

3.1. Analytical Measurements. All the chemicals used in synthesis are analytically pure and were used as received. Solvents were dried and distilled before use for synthesis. Luminescence lifetimes were measured on a OB 920 fluorescence/phosphorescence lifetime spectrofluorometer (Edinburgh Instruments, UK). Luminescence quantum yields of the compounds were measured with **A-1** as the standard (Φ_F = 0.98 in *n*-hexane).

3.2. Synthesis of 1. Compound **1** was prepared by the reported method.[46] **A-1** (1.51 g, 6.0 mmol) and DMF (180 mL) were mixed, and the mixture was stirred at room temperature until all perylene solid was dissolved. Then DMF (20 mL) solution of *N*-bromosuccinimide (1.05 g, 6.0 mmol) was slowly added, and the solution was stirred for 24 h at room temperature. H_2O was added to the reaction mixture to give a golden solid, which was collected by filtration. The crude solid is 3-bromoperylene (1.75 g, yield 84%). This compound was used directly for the next reaction. TOF HRMS ESI^-: Calcd ($[C_{20}H_{11}Br]^+$), *m*/*z* = 330.0044, found, *m*/*z* = 330.0053.

3.3. Synthesis of A-2. Under Ar atmosphere, 3-bromoperylene (230.0 mg, 0.70 mmol), phenylboronic acid (85.4 mg, 0.70 mmol), K_2CO_3 (290.0 mg, 2.1 mmol), and EtOH/toluene/water (v/v/v = 2:2:1, 50 mL) were mixed together. Then $Pd(PPh_3)_4$ (40.4 mg, 0.035 mmol, 5.0 mol %) was added. The reaction mixture were refluxed and stirred under Ar for 8 h. After completion of the reaction, the mixture was cooled to room temperature. The reaction mixture was extracted with CH_2Cl_2, and the organic layer was washed with water (2 × 100 mL) and dried over Na_2SO_4. The solution was evaporated to dryness

dx.doi.org/10.1021/jo402718e | J. Org. Chem. 2014, 79, 2038−2048

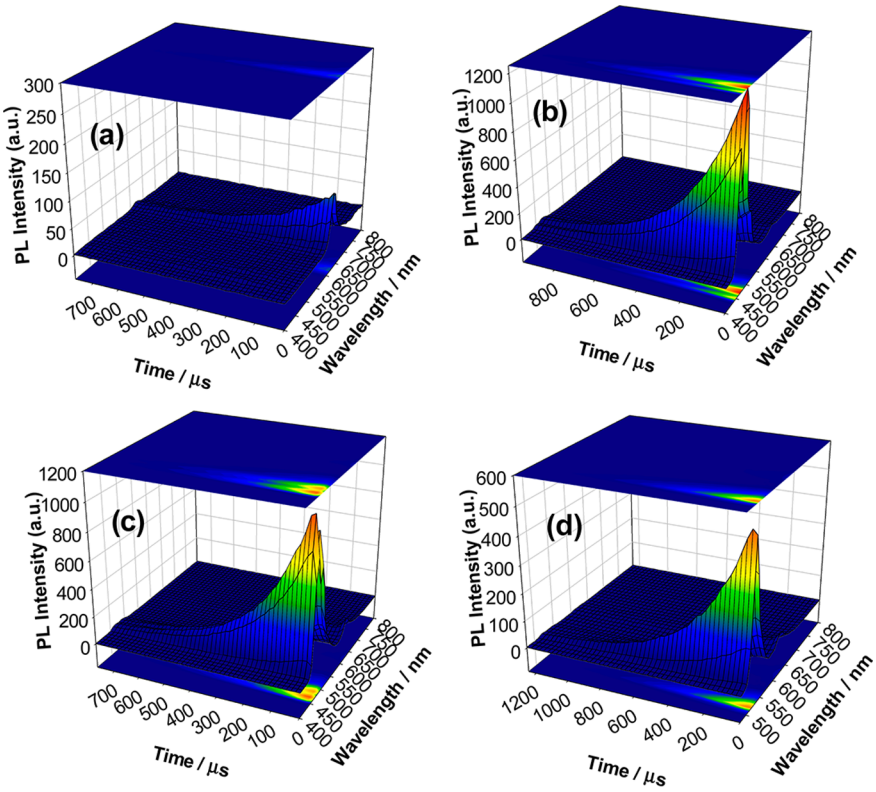

Figure 9. Time-resolved emission spectra (TRES) of the TTA assisted upconversion **A-1**, **A-2**, and **A-3** as the triplet acceptor. (a) **B-6** alone. τ_F = 92.0 μs (λ_{em} = 630 nm). (b) **B-6**/**A-1**, τ_{DF} = 241.2 μs (λ_{em} = 450 nm). (c) **B-6**/**A-2**, τ_{DF} = 195.7 μs (λ_{em} = 460 nm). (d) **B-6**/**A-3**, τ_{DF} = 284.1 μs (λ_{em} = 520 nm). The samples were excited using nanosecond pulsed OPO laser (589 nm). *c* [**B-6**] = 2.0 × 10^{-6} M. *c* [Acceptor] = 4.0 × 10^{-5} M. In deaerated toluene, 20 °C.

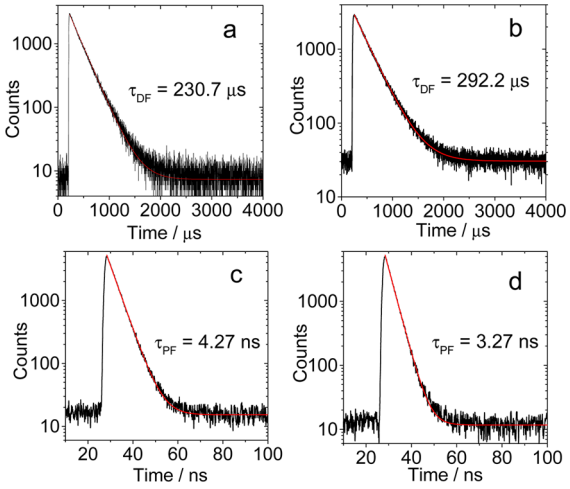

Figure 10. Delayed fluorescence observed in the TTA assisted upconversion with **B-6** as the triplet photosensitizer and (a) **A-1**, (b) **A-3** as the triplet acceptor. Excited at 589 nm (nanosecond pulsed OPO laser, synchronized with FLS 920 spectrofluorometer), the emission was monitored at 445 nm (**A-1**) and 520 nm (**A-3**). The decay trace of the prompt fluorescence of (c) **A-1** and (d) **A-3** determined in a different experiment. Excited with picosecond pulsed 405 nm laser; the decay of the emission was monitored at 445 nm (**A-1**) and 520 nm (**A-3**). In deaerated toluene; *c* [**B-6**] = 2.0 × 10^{-6} M; *c* [Acceptor] = 4.0 × 10^{-5} M, 20 °C.

under reduced pressure to obtain a crude solid. The crude product was further purified with column chromatography (silica gel, CH_2Cl_2/petroleum ether = 1:10, v/v) to give orange solid (164.1 mg, Yield: 72%). Mp, 196–199 °C. ^{1}H NMR ($CDCl_3$, 400 MHz): δ 8.26–8.21

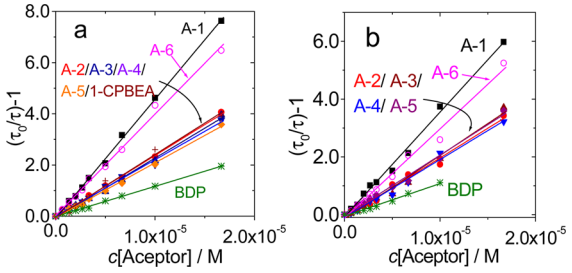

Figure 11. Stern–Volmer plot of quenching of the triplet state of (a) **B-6** and (b) PdTPTBP with different triplet acceptor. *c*[triplet photosensitizer] = 2.0 × 10^{-6} M. In deaerated toluene, 20 °C.

(m, 4H), 7.78 (d, 1H, *J* = 12.0 Hz), 7.71 (d, 2H, *J* = 8.0 Hz), 7.53–7.48 (m, 6H), 7.45 (t, 3H, *J* = 12.0 Hz). ^{13}C NMR (100 MHz, $CDCl_3$) δ 140.9, 140.2, 134.9, 133.1, 131.6, 131.4, 130.8, 130.1, 129.3, 128.9, 128.6, 127.9, 127.5, 126.8, 126.7, 126.3, 120.5, 120.3, 120.1. TOF HRMS ESI$^-$: Calcd ($[C_{26}H_{16}]^+$), *m*/*z* = 328.1252, found, *m*/*z* = 328.1261.

3.4. Synthesis of A-3. **A-3** was obtained following procedure similar to that of **A-2**. 3-Bromoperylene (100.0 mg, 0.30 mmol), **2** (135.4 mg, 0.30 mmol) instead of phenylboronic acid, K_2CO_3 (124.2 mg, 0.9 mmol), and $Pd(PPh_3)_4$ (17.3 mg, 0.015 mmol, 5 mol %) were mixed in EtOH/toluene/water (v/v/v = 2:2:1, 50 mL). After the reaction finished, the crude product was further purified with column chromatography (silica gel, CH_2Cl_2/petroleum ether = 1:2, v/v) to give red solid (70.2 mg, Yield: 40%). Mp > 250 °C. ^{1}H NMR ($CDCl_3$, 400 MHz): δ 8.28 (d, 2H, *J* = 8.0 Hz), 8.25 (d, 2H, *J* = 8.0 Hz), 7.73 (d, 3H, *J* = 6.4 Hz), 7.67 (d, 2H, *J* = 7.6 Hz), 7.52–7.43 (m, 6H), 6.05 (s, 2H), 2.59 (s, 6H), 1.58 (s, 6H). ^{13}C NMR (100 MHz, $CDCl_3$): δ 155.8, 143.2, 141.8, 141.7, 139.0, 131.4, 130.9, 129.0, 128.8, 128.7, 128.3, 127.0, 126.9, 125.6, 121.5, 120.7, 120.6, 120.5, 120.0, 19.4, 14.8.

dx.doi.org/10.1021/jo402718e | J. Org. Chem. 2014, 79, 2038–2048

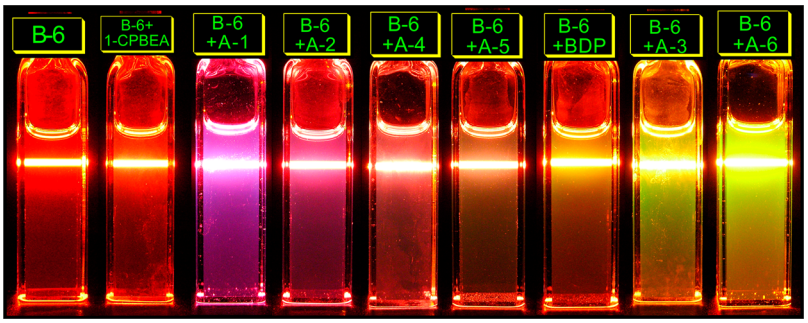

Figure 12. Photographs of the emission of triplet photosensitizer (**B-6**) alone and the TTA assisted upconversion. Excited with 589 nm laser (4.8 mW). The use of different triplet acceptors is marked. c [**B-6**] = 2.0 × 10^{-6} M; c [acceptor] = 4.0 × 10^{-5} M; in deaerated toluene, 20 °C.

TOF HRMS ESI⁻: Calcd ($[C_{39}H_{29}BF_2N_2]^+$), m/z = 574.2392, found, m/z = 574.2407.

3.5. Synthesis of A-4. 3-Bromoperylene (60.0 mg, 0.18 mmol), 1-ethynylbenzene (0.19 mL, 1.8 mmol), toluene (10 mL), and triethylamine (10 mL) were mixed together. Then $Pd(PPh_3)_2Cl_2$ (12.6 mg, 0.018 mmol, 10 mol %), PPh_3 (4.7 mg, 0.018 mmol 10 mol %), and CuI (3.4 mg, 0.018 mmol, 10 mol %) were added. The reaction mixture was refluxed at 90 °C and stirred under Ar for 8 h. After completion of the reaction, the mixture was cooled to rt and the yellow precipitate was collected by filtration. Then the crude product was purified with column chromatography (silica gel, CH_2Cl_2/petroleum ether = 1:10, v/v) to give 35.0 mg yellow solid (Yield: 55%). Mp > 250 °C. ^{1}H NMR ($CDCl_3$, 400 MHz): δ 8.33 (d, 1H, J = 8.0 Hz), 8.28 (d, 1H, J = 7.2 Hz), 8.24 (t, 2H, J = 14.4 Hz), 8.19 (d, 1H, J = 8.0 Hz), 7.77 (d, 1H, J = 7.6 Hz), 7.73−7.65 (m, 4H), 7.63 (t, 1H, J = 8.0 Hz), 7.53 (t, 2H, J = 12.0 Hz), 7.42−7.38 (m, 3H). ^{13}C NMR (100 MHz, $CDCl_3$) δ 134.8, 132.0, 131.8, 131.2, 131.0, 130.8, 128.6, 127.4, 126.8, 126.4, 121.1, 120.5, 119.9, 95.6, 88.2. TOF HRMS ESI⁻: Calcd ($[C_{28}H_{16}]^+$), m/z = 352.1252, found, m/z = 352.1248.

3.6. Synthesis of A-5. **A-5** was obtained following a procedure similar to that of **A-4** except 9-butyl-3-ethynyl-carbazole (**3**) (60.0 mg, 0.24 mmol) was used. The crude product was purified with column chromatography (silica gel, CH_2Cl_2/petroleum ether = 1:3, v/v) to give 42.3 mg yellow solid (Yield: 47%). Mp, 241−244 °C. ^{1}H NMR ($CDCl_3$, 400 MHz): δ 8.44 (d, 2H, J = 8.0 Hz), 8.29−8.15 (m, 5H), 7.80 (t, 2H, J = 19.2 Hz), 7.72 (d, 2H, J = 8.0 Hz), 7.66 (t, 1H, J = 8.0 Hz), 7.53 (t, 3H, J = 15.2 Hz), 7.45−7.42 (m, 2H), 7.29 (s, 1H), 4.36 (t, 2H, J = 14.0 Hz), 1.91 (t, 2H, J = 14.4 Hz), 1.46 (q, 2H, J = 22.8 Hz), 0.99 (t, 3H, J = 14.8 Hz). ^{13}C NMR (100 MHz, $CDCl_3$) δ 141.0, 140.4, 134.8, 126.8, 126.6, 126.3, 124.2, 123.1, 122.7, 121.3, 120.9, 120.8, 120.7, 120.0, 119.6, 113.5, 109.2, 109.0, 97.3, 86.5, 43.2, 31.3, 20.8, 14.1. TOF HRMS ESI⁻: Calcd ($[C_{38}H_{27}N]^+$), m/z = 497.2143, found, m/z = 497.2144.

3.7. Triplet−Triplet Annihilation Assisted Upconversions. Diode pumped solid state (DPSS) continuous lasers with 589 nm (type MGL-III, laser power is tunable in the range of 1−50 mW. Changchun New Industries Optoelectronics Tech. Co., Ltd., China) and 635 nm (type T635D500, laser power is tunable in the range of 1−500 mW. Xi'an Minghui Optoelectronic Technology Co., Ltd., China) output were used for the upconversion. The diameter of the 589 nm laser spot is ca. 5 mm, and for the 635 nm laser, it is ca. 6 mm. The power of the laser beam was measured with VLP-2000 pyroelectric laser power meter. For the upconversion experiments, the mixed solution (with different triplet sensitizer and acceptor) was degassed for at least 15 min with N_2 before measurement, and the gas flow is maintained during the measurement. Then, the solution was excited with laser. The upconverted fluorescence was recorded with a RF 5301PC spectrofluorometer. In order to reduce the scattered laser, a black box was put behind the fluorescent cuvette to damp the laser beam.

The upconversion quantum yields (Φ_{UC}) of **B-6** and **PdTPTBP** were determined with the prompt fluorescence of compound **B-6** (Φ_F = 10.5%, in toluene) and **H_2TPTBP** (Φ_F = 0.28%, in toluene) as the inner standard. The upconversion quantum yields were calculated with the following equation, where Φ_{UC}, A_{sam}, I_{sam}, and η_{sam} represent the quantum yield, absorbance, integrated photoluminescence intensity, and the refractive index of the samples and the solvents (eq 1, where the subscript "std" is for the standard used in the measurement of the quantum yield and "sam" for the samples to be measured). The equation is multiplied by a factor of 2 in order to make the maximum quantum yield unity.

$$\Phi_{UC} = 2\Phi_{std}\left(\frac{A_{std}}{A_{sam}}\right)\left(\frac{I_{sam}}{I_{std}}\right)\left(\frac{\eta_{sam}}{\eta_{std}}\right)^2 \quad (1)$$

The TTET efficiency was obtained through the Stern−Volmer quenching constants, the concentration of the photosensitizer was fixed, the lifetime of the photosensitizers was measured by LP920 laser flash photolysis spectrometer with increasing perylene concentration in the solution.

3.8. Nanosecond Time-Resolved Transient Difference Absorption Spectra. The nanosecond time-resolved transient difference absorption spectra were measured on LP920 laser flash photolysis spectrometer (Edinburgh Instruments, UK) and recorded on a Tektronix TDS 3012B oscilloscope. The lifetime values (by monitoring the decay trace of the transients) were obtained with the LP900 software. All samples in flash photolysis experiments were deaerated with N_2 for ca. 15 min before measurement and the gas flow is kept during the measurement.

3.9. Delayed Fluorescence of the Upconversion. The spectra were measured with a nanosecond pulsed laser (OpoletteTM 355II +UV nanosecond pulsed laser, typical pulse length: 7 ns. Pulse repetition: 20 Hz. Peak OPO energy: 4 mJ. The wavelength is tunable in the range of 210−355 nm and 410−2200 nm. OPOTEK, USA), which is synchronized to FLS 920 spectrofluorometer (Edinburgh Instruments, UK). The decay kinetics of the upconverted fluorescence (delayed fluorescence) was monitored with an FLS920 spectrofluorometer (synchronized to the OPO nanosecond pulse laser). The prompt fluorescence lifetime of the triplet acceptor was measured with EPL picosecond pulsed laser (405 nm, 405 ± 10 nm, pulse width: 66.9 ps, maximum average power: 5 mW; Edinburgh Instrument Ltd., UK) which was synchronized to the FLS 920 spectrofluorometer.

3.10. Cyclic Voltammetry. Cyclic voltammetry was performed using a CHI610D Electrochemical workstation (Shanghai, China). Cyclic voltammograms were recorded at scan rates of 0.1 V/s. The electrolytic cell used was a three electrodes cell. Electrochemical measurements were performed at RT using 0.1 M tetrabutylammonium hexafluorophosphate ($Bu_4N[PF_6]$) as supporting electrolyte, after purging with N_2. The working electrode was a glassy carbon electrode, and the counter electrode was platinum electrode. A nonaqueous $Ag/AgNO_3$ (0.1 M in acetonitrile) reference electrode was contained in a separate compartment connected to the solution via frit. DCM was used as the solvent. Ferrocene was added as the internal reference.

3.11. DFT Calculations. TD-DFT was used to probe the nature of the excited states of the dyads. All calculations have been performed with the Gaussian 09 program,[56] without performing any structural simplification. We have applied the computational protocol recently

dx.doi.org/10.1021/jo402718e | J. Org. Chem. 2014, 79, 2038−2048

optimized for BODIPY derivatives,[57a] and we redirect the interested reader to that earlier contribution for a complete discussion of methodological aspects. Our protocol relies on the M06-2X[58] exchange-correlation functional for all computational steps, as it is known that this hybrid meta-GGA is adequate for excited-state calculations.[59] The 6-31G(d) atomic basis set is used to determine geometrical and vibrational parameters, whereas a much more extended basis set, 6-311+G(2d,p), is used to correct the computed 0−0 energies. This basis set combination yields nearly converged transition energies for BODIPY derivatives.[60] The ground and excited-state structures have been optimized using analytic DFT and TD-DFT gradients, respectively. These force minimizations have been performed until the residual mean square force is smaller than 1×10^{-5} a.u. (tight threshold in Gaussian09). The harmonic vibrational frequencies of the optimized structures have been computed on the optimal geometries using analytic and numerical differentiation for ground and excited states, respectively. This allowed us to ascertain the nature of the minima. In our calculations, the electrostatic interactions between the compound and the environment have been modeled thanks to the PCM method that restores valid solvent effect, as long as no specific solute−solvent interactions take place.[61] For this reason, we have modeled the results in toluene here. Both absorption and fluorescence maxima have been evaluated using the state-specific (SS) PCM model that allows correct polarization of the excited-state cavity.[62] Therefore, the reported 0−0 energies account for both state-specific solvation and vibrational effects. The vibrationally resolved spectra—within the harmonic approximation—were computed using the FCclasses program.[63,64] The reported spectra have been simulated using a convoluting Gaussian function presenting a full width at half-maximum (fwhm) of 0.07 eV. A maximal number of 25 overtones for each mode and 20 combination bands on each pair of modes were included in the calculation. The maximum number of integrals to be computed for each class was set to 1×10^{10}, and it was checked that such numbers provide converged FC factors (>0.9; see discussion in ref 64 and references therein).

■ ASSOCIATED CONTENT

Supporting Information

Free energy calculations, molecular structure characterization data (NMR, HRMS spectra) and UV−vis spectra, cyclovoltammetric graph, TTA assisted upconversion graphs, and tables of atom coordinates and absolute energies. This material is available free of charge via the Internet at http://pubs.acs.org.

■ AUTHOR INFORMATION

Corresponding Authors

*E-mail: zhaojzh@dlut.edu.cn. Web: http://finechem.dlut.edu.cn/photochem.

*E-mail: Denis.Jacquemin@univ-nantes.fr. Fax: (+33) 251 125 40.

Notes

The authors declare no competing financial interest.

■ ACKNOWLEDGMENTS

J. Z. thanks the NSFC (21073028 and 21273028), the Royal Society (UK) and NSFC (China-UK Cost-Share Science Networks, 21011130154), Ministry of Education (NCET-08-0077 and SRFDP-20120041130005) and Dalian University of Technology for financial support. A. C. E. and D. J. acknowledge the European Research Council (ERC) for financial support in the framework of Starting Grant (Marches-278845). This research used resources of the GENCI-CINES/IDRIS, of the CCIPL (*Centre de Calcul Intensif des Pays de Loire*) and of a local Troy cluster.

■ REFERENCES

(1) Baluschev, S.; Miteva, T.; Yakutkin, V.; Avlasevich, Y.; Nelles, G.; Cheprakov, A.; Yasuda, A.; Wegner, G. *Phys. Rev. Lett.* **2006**, *97*, 143903.

(2) Singh-Rachford, T. N.; Castellano, F. N. *Coord. Chem. Rev.* **2010**, *254*, 2560−2573.

(3) Zhang, C.; Zheng, J.; Zhao, Y.; Yao, J. *Adv. Mater.* **2011**, *23*, 1380−1384.

(4) Chow, P. K.; Ma, C.; To, W. P.; Tong, G. S. M.; Lai, S. L.; Kui, S. C. F.; Kwok, W. M.; Che, C. M. *Angew. Chem., Int. Ed.* **2013**, *52*, 6648−6652.

(5) Zhao, J.; Ji, S.; Guo, H. *RSC Adv.* **2011**, *1*, 937−950.

(6) Cerono, P. *Chem.—Eur. J.* **2011**, *17*, 9560−9564.

(7) Monguzzi, A.; Tubino, R.; Hoseinkhani, S.; Campione, M.; Meinardi, F. *Phys. Chem. Chem. Phys.* **2012**, *14*, 4322−4332.

(8) Simon, Y. C.; Weder, C. *J. Mater. Chem.* **2012**, *22*, 20817−20830.

(9) Mani, T.; Vinogradov, S. A. *J. Phys. Chem. Lett.* **2013**, *4*, 2799−2804.

(10) Ji, S.; Guo, H.; Wu, W.; Wu, W.; Zhao, J. *Angew. Chem., Int. Ed.* **2011**, *50*, 8283−8286.

(11) Ji, S.; Wu, W.; Wu, W.; Guo, H.; Zhao, J. *Angew. Chem., Int. Ed.* **2011**, *50*, 1626−1629.

(12) Monguzzi, A.; Tubino, R.; Meinardi, F. *Phys. Rev. B* **2008**, *77*, 155122/1−155122/4.

(13) Haase, M.; Schäfer, H. *Angew. Chem., Int. Ed.* **2011**, *50*, 5808−5829.

(14) Adikaari, A. A. D.; Etchart, I.; Guéring, P.-H.; Bérard, M.; Silva, S. R. P.; Cheetham, A. K.; Curry, R. J. *J. Appl. Phys.* **2012**, *111*, 094502.

(15) Liu, Q.; Sun, Y.; Yang, T.; Feng, W.; Li, C.; Li, F. *J. Am. Chem. Soc.* **2011**, *133*, 17122−17125.

(16) Wenger, O. S.; Güdel, H. U. *Inorg. Chem.* **2001**, *40*, 5747−5753.

(17) Lüthi, S. R.; Pollnau, M.; Güdel, H. U.; Hehlen, M. P. *Phys. Rev. B* **1999**, *60*, 162−178.

(18) Kim, J.-H.; Kim, J.-H. *J. Am. Chem. Soc.* **2012**, *134*, 17478−17481.

(19) Liu, Q.; Yang, T.; Feng, W.; Li, F. *J. Am. Chem. Soc.* **2012**, *134*, 5390−5397.

(20) Borisov, S. M.; Larndorfer, C.; Klimant, I. *Adv. Funct. Mater.* **2012**, *22*, 4360−4368.

(21) Cheng, Y. Y.; Fückel, B.; MacQueen, R. W.; Khoury, T.; Clady, R. G. C. R.; Schulze, T. F.; Ekins-Daukes, N. J.; Crossley, M. J.; Stannowski, B.; Lips, K. *Energy Environ. Sci.* **2012**, *5*, 6953−6959.

(22) Schulze, T. F.; Czolk, J.; Cheng, Y.-Y.; Fückel, B.; MacQueen, R. W.; Khoury, T.; Crossley, M. J.; Stannowski, B.; Lips, K.; Lemmer, U. *J. Phys. Chem. C* **2012**, *116*, 22794−22801.

(23) Börjesson, K.; Dzebo, D.; Albinsson, B.; Moth-Poulsen, K. *J. Mater. Chem. A* **2013**, *1*, 8521−8524.

(24) Khnayzer, R. S.; Blumhoff, J.; Harrington, J. A.; Haefele, A.; Deng, F.; Castellano, F. N. *Chem. Commun.* **2011**, *48* (2), 209−211.

(25) Moor, K.; Kim, J.-H.; Snow, S.; Kim, J.-H. *Chem. Commun.* **2013**, *49*, 10829−10831.

(26) Liang, Z.-Q.; Sun, B.; Ye, C.-Q.; Wang, X.-M.; Tao, X.-T.; Wang, Q.-H.; Ding, P.; Wang, B.; Wang, J.-J. *ChemPhysChem* **2013**, *14*, 3517−3522.

(27) Zhao, J.; Wu, W.; Sun, J.; Guo, S. *Chem. Soc. Rev.* **2013**, *42*, 5323−5351.

(28) Turshatov, A.; Busko, D.; Avlasevich, Y.; Miteva, T.; Landfester, K.; Baluschev, S. *ChemPhysChem* **2012**, *13*, 3112−3115.

(29) Singh-Rachford, T. N.; Haefele, A.; Ziessel, R.; Castellano, F. N. *J. Am. Chem. Soc.* **2008**, *130*, 16164−16165.

(30) Cao, X.; Hu, B.; Zhang, P. *J. Phys. Chem. Lett.* **2013**, *4*, 2334−2338.

(31) Chen, H.-C.; Hung, C.-Y.; Wang, K.-H.; Chen, H.-L.; Fann, W. S.; Chien, F.-C.; Chen, P.; Chow, T. J.; Hsu, C.-P.; Sun, S.-S. *Chem. Commun.* **2009**, 4064−4066.

(32) Bergamini, G.; Ceroni, P.; Fabbrizi, P.; Cicchi, S. *Chem. Commun.* **2011**, *47*, 12780−12782.

(33) Moor, K.; Kim, J.-H.; Snow, S.; Kim, J. *Chem. Commun.* **2013**, *49*, 3537−3539.

(34) Du, P.; Eisenberg, R. *Chem. Sci.* **2010**, *1*, 502−506.
(35) Dayan, S.; Ozpozan Kalaycioglu, N.; Daran, J. C.; Labande, A.; Poli, R. *Inorg. Chem.* **2013**, *52*, 1206−1216.
(36) Deng, F.; Sommer, J.; Myahkostupov, M.; Schanze, K.; Castellano, F. N. *Chem. Commun.* **2013**, *49*, 7406−7408.
(37) Huang, D.; Sun, J.; Ma, L.; Zhang, C.; Zhao, J. *Photochem. Photobiol. Sci.* **2013**, *12*, 872−882.
(38) Cortijo, M.; González-Prieto, R.; Herrero, S.; Jiménez-Aparicio, R.; Sánchez Rivera, P. *Inorg. Chem.* **2013**, *52*, 6299−6310.
(39) Wu, W.; Zhao, J.; Sun, J.; Huang, L.; Yi, X. *J. Mater. Chem. C* **2013**, *1*, 705−716.
(40) Guo, S.; Sun, J.; Ma, L.; You, W.; Yang, P.; Zhao, J. *Dyes Pigm.* **2013**, *96*, 449−458.
(41) Huang, D.; Zhao, J.; Wu, W.; Yi, X.; Yang, P.; Ma, J. *Asian J. Org. Chem.* **2012**, *1*, 264−273.
(42) Yang, P.; Wu, W.; Zhao, J.; Huang, D.; Yi, X. *J. Mater. Chem.* **2012**, *22*, 20273−20283.
(43) Wu, W.; Zhao, J.; Sun, J.; Guo, S. *J. Org. Chem.* **2012**, *77*, 5305−5312.
(44) Singh-Rachford, T. N.; Nayak, A.; Muro-Small, M. L.; Goeb, S.; Therien, M. J.; Castellano, F. N. *J. Am. Chem. Soc.* **2010**, *132*, 14203−14211.
(45) Adachi, M.; Nagao, Y. *Chem. Mater.* **2001**, *13*, 662−669.
(46) Yamaji, M.; Maeda, H.; Nanai, Y.; Mizuno, K. *Chem. Phy. Let.* **2012**, *536*, 72−76.
(47) Shao, J.; Guo, H.; Ji, S.; Zhao, J. *Biosensors Bioelectron.* **2011**, *26*, 3012−3017.
(48) Ulrich, G.; Ziessel, R.; Harriman, A. *Angew. Chem., Int. Ed.* **2008**, *47*, 1184−1201.
(49) Loudet, A.; Burgess, K. *Chem. Rev.* **2007**, *107*, 4891−4932.
(50) Kamkaew, A.; Lim, S. H.; Lee, H. B.; Kiew, L. V.; Chung, L. Y.; Burgess, K. *Chem. Soc. Rev.* **2013**, *42*, 77−88.
(51) Benniston, A. C.; Copley, G. *Phys. Chem. Chem. Phys.* **2009**, *11*, 4124−4131.
(52) Coskun, A.; Akkaya, E. U. *J. Am. Chem. Soc.* **2006**, *128*, 14474−14475.
(53) Kostereli, Z.; Ozdemir, T.; Buyukcakir, O.; Akkaya, E. U. *Org. Lett.* **2012**, *14*, 3636−3639.
(54) Brizet, B.; Eggenspiller, A.; Gros, C. P.; Barbe, J.-M.; Goze, C.; Denat, F.; Harvey, P. D. *J. Org. Chem.* **2012**, *77*, 3646−3650.
(55) Dance, Z. E. X.; Mickley, S. M.; Wilson, T. M.; Ricks, A. B.; Scott, A. M.; Ratner, M. A.; Wasielewski, M. R. *J. Phys. Chem. A* **2008**, *112*, 4194−4201.
(56) Frisch, M. J.; Trucks, G. W.; Schlegel, H. B.; Scuseria, G. E.; Robb, M. A.; Cheeseman, J. R.; Scalmani, G.; Barone, V.; Mennucci, B.; Petersson, G. A.; Nakatsuji, H.; Caricato, M.; Li, X.; Hratchian, H. P.; Izmaylov, A. F.; Bloino, J.; Zheng, G.; Sonnenberg, J. L.; Hada, M.; Ehara, M.; Toyota, K.; Fukuda, R.; Hasegawa, J.; Ishida, M.; Nakajima, T.; Honda, Y.; Kitao, O.; Nakai, H.; Vreven, T.; Montgomery, J. A., Jr.; Peralta, J. E.; Ogliaro, F.; Bearpark, M.; Heyd, J. J.; Brothers, E.; Kudin, K. N.; Staroverov, V. N.; Kobayashi, R.; Normand, J.; Raghavachari, K.; Rendell, A.; Burant, J. C.; Iyengar, S. S.; Tomasi, J.; Cossi, M.; Rega, N.; Millam, J. M.; Klene, M.; Knox, J. E.; Cross, J. B.; Bakken, V.; Adamo, C.; Jaramillo, J.; Gomperts, R.; Stratmann, R. E.; Yazyev, O.; Austin, A. J.; Cammi, R.; Pomelli, C.; Ochterski, J. W.; Martin, R. L.; Morokuma, K.; Zakrzewski, V. G.; Voth, G. A.; Salvador, P.; Dannenberg, J. J.; Dapprich, S.; Daniels, A. D.; Ö. Farkas, Foresman, J. B.; Ortiz, J. V.; Cioslowski, J.; Fox, D. J., *Gaussian 09*, revision D.01; Gaussian Inc., Wallingford, CT, 2009.
(57) (a) Chibani, S.; Le Guennic, B.; Charaf-Eddin, A.; Laurent, A. D.; Jacquemin, D. *Chem. Sci.* **2013**, *4*, 1950−1963. (b) Quartarolo, A. D.; Russo, N.; Sicilia., E. *Chem.—Eur. J.* **2006**, *12*, 6797−6803.
(58) Zhao, Y.; Truhlar, D. G. *Theor. Chem. Acc.* **2008**, *120*, 215−241.
(59) See a recent review Laurent, A. D.; Jacquemin, D. *Int. J. Quantum Chem.* **2013**, *113*, 2019−2039 and refs therein.
(60) Chibani, S.; Le Guennic, B.; Charaf-Eddin, A.; Maury, O.; Andraud, C.; Jacquemin, D. *J. Chem. Theory Comput.* **2012**, *8*, 3303−3313.
(61) Tomasi, J.; Mennucci, B.; Cammi, R. *Chem. Rev.* **2005**, *105*, 2999−3094.
(62) Improta, R.; Barone, V.; Scalmani, G.; Frisch, M. J. *J. Chem. Phys.* **2006**, *125*, 054103−054109.
(63) Santoro, F.; Improta, R.; Lami, A.; Bloino, J.; Barone, V. *J. Chem. Phys.* **2007**, *126*, 084509.
(64) Santoro, F.; Lami, A.; Improta, R.; Barone, V. *J. Chem. Phys.* **2007**, *126*, 184102.
(65) Charaf-Eddin, A.; Planchat, A.; Mennucci, B.; Adamo, C.; Jacquemin, D. *J. Chem. Theory Comput.* **2013**, *9*, 2749−2760.
(66) Cheng, Y. Y.; Khoury, T.; Clady, R. G. C. R.; Tayebjee, M. J. Y.; Ekins-Daukes, N. J.; Crossley, M. J.; Schmidt, T. W. *Phys. Chem. Chem. Phys.* **2010**, *12*, 66−71.
(67) Kim, J.-H.; Deng, F.; Castellano, F. N.; Kim, J.-H. *Chem. Mater.* **2012**, *24*, 2250.